Available online at www.elixirpublishers.com (Elixir International Journal)

Vibrational Spectroscopy

Elixir Vib. Spec. 92 (2016) 38706-38717

ISSN: 2229-712X

Ab initio Hartee-Fock and density functional theory studies on, 4-Acetyl-N-(4-methoxybenzylidene)aniline

F.Liakath Ali Khan[1], G.Saravanan[2,*] and A.Md.Sabeelullah Roomy[3]
Department of Physics, Islamiah College (Autonomous), Vaniyambadi, India.

ARTICLE INFO

Article history:
Received: 3 February 2016;
Received in revised form:
29 February 2016;
Accepted: 2 March 2016;

Keywords
4A-N-(4MB)A,
HOMO,
LUMO,
NBO and TED.

ABSTRACT
The optimized molecular structure, vibrational frequencies, corresponding vibrational assignments and thermodynamic properties of 4-Acetyl-N-(4-methoxybenzylidene)aniline [4A-N-(4MB)A] have been investigated by using *ab initio* HF/6-311++G(d,p) and DFT/B3LYP method at 6-311G(d,p) and 6-311++G(d,p) basis sets. The energy and oscillator strength calculated by TD-DFT are in line with experimental findings. The ^{1}H and ^{13}C NMR chemical shifts calculations of the 4A-N-(4MB)A molecule were carried out by using HF/6-311++G(d,p) and B3LYP functional with 6-311G(d,p)/6-311++G(d,p) basis set. HOMO and LUMO orbitals have been visualized. The stability of the molecule arising from hyperconjugative interaction and charge delocalization has been analyzed using natural NBO analysis. The minimum energy conformational analysis was carried out with the help of PES scan. Besides, MEP was calculated and Mulliken charges, IR and Raman intensities have also been reported.

1. Introduction

The title compound 4A-N-(4MB)A is a curcumin derivative. Curcumin is a natural polyphenol derived from the plant Curcumalonga, which has been used in the Indian Ayurveda medicine. Extensive researches reveal that curcumin exhibits a remarkable range of pharmacological activities, such as antioxidant, anti-viral, and anti-tutor activities [1, 2]. Recent research also indicated that these pharmacological actions of curcumin may owe to its inhibition against cellular glyoxalases. Enzyme kinetics studies reveal that curcumin elicits a significant inhibitory activity on GLOI (Ki=5.1 μM) [3]. Curcumins have several biological activities, such as anti-inflammatory, antioxidative, antibacterial, antihepatotoxic, hypertensive and hypocholesterolenic properties [4–8]. Curcumin inhibits *in vitro* lipid peroxide formation by liver homogenates of endemic mice [9]. It is used for the synthesis of bioactive pyrimidine compounds [10] and also finds applications in the preparation of liquid-crystalline polymers [11].

Thermo tropic liquid crystalline behavior of polymeric materials containing cyclopentanone moiety linked with polyethylene spacers is of considerable current interest, not only because of their potential as high-strength fibers, plastics, moldings, etc. [12–14], but also their applications in non-linear optical materials [15]. The benzylidene derivatives are intermediates in various pharmaceuticals, agrochemicals and perfumes [16]. Curcumin demonstrated a great ability in chelating essential metal ions such as Cu(II) [17] and the complexes showed a higher scavenging ability than curcumin.

Fluorescence Quenching studies of curcumin by hydrogen peroxide in Acetonitrile solution is reported by Iwunze [18]. E. Benassi et al., [19] carried out a theoretical study about the structural, electronic and spectroscopic properties of the ground and single excited states of curcuminoidic core concerning the ground state, tautomeric equilibrium, vibrational and therochemical analysis; and electronic absorption spectra (with *ab initio* and semi-empirical methodologies) have been studied. A full geometry optimization of the first singlet excited states was obtained, with different computational methodologies.

An investigation of NMR spectra of Dihydropyridones derived from curcumin is conducted by Bahjat et al., [20]. ^{1}H and ^{13}C NMR spectra of dihydropyridones derived from curcumin were discussed and their structures were elucidated accordingly. The optimized structure is used to calculate the NMR chemical shifts at the B3LYP/6-311G(d,p) level using the GIAO method. Comparative anti-inflammatory activities of Curcumin and Tetrahydrocurcumin are analyzed by Yukio et al., [21]. In addition, the bond dissociation enthalpy of the phenolic OH was calculated using the DFT/B3LYP.

Literature survey reveals that to the best of our knowledge, *ab initio* HF, DFT calculations and experimental studies on 4A-N-(4MB)A molecule have not been reported so far. Therefore, The present work deals with FT-IR and FT-Raman spectroscopic investigation of 4A-N-(4MB)A utilizing HF/6-311++G(d,p) and DFT method with 6-311G(d,p)/6-311++G(d,p) as basis sets. The UV and NMR spectral studies have been carried out by using TD-DFT/B3LYP/6-311++G(d,p) and HF/6-311++G(d,p), B3LYP/6-311G(d,p)/6-311++G(d,p) basis sets respectively. Vibrational spectrum of the molecule is supported by using the SQM force field technique based on DFT. The redistribution of ED in various bonding and anti-bonding orbitals and E2 energies has been calculated by NBO analysis using DFT method. The HOMO and LUMO analysis have been used to elucidate information regarding charge transfer within the molecule.

Tele:
E-mail address: saravanangandhi78@gmail.com

2. Experimental Details

The FT-Raman spectrum of 4A-N-(4MB)A was recorded using the 1064 nm line of a Nd:YAG laser as excitation wavelength in the region 10-3500 cm^{-1} on a Brucker model IFS 66V spectrophotometer equipped with an FRA 106 FT-Raman module accessory. The FT-IR spectrum of this compound was recorded in the region 400-4000 cm^{-1} on an IFS 66V spectrophotometer using the KBr pellet technique. The spectrum was recorded at room temperature, with a scanning speed of 10 cm^{-1} per minute and at the spectral resolution of 2.0 cm^{-1}. The theoretically predicted IR and Raman spectra at HF/6-311++G(d,p) and B3LYP/6-311G(d,p)/6-311++G(d,p) level of calculations are shown in Figs.1 and 2 respectively along with the experimental spectrum.

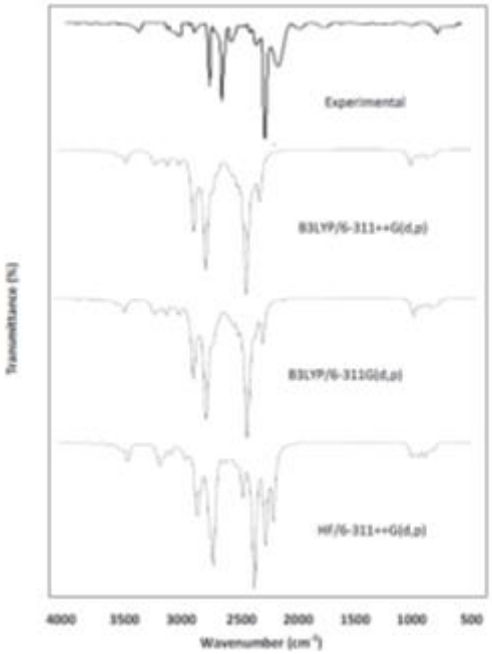

Fig 1. Comparison of the Experimental and computed FT-IR spectra of 4A-N-(4MB)A

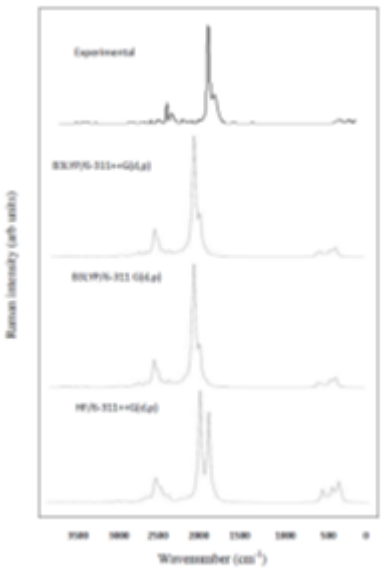

Fig 2. Comparison of the Experimental and computed FT-Raman spectra of 4A-N-(4MB)A

3. Computational Details

For meeting the requirements of both accuracy and computing economy, theoretical methods and basis sets should be considered. DFT has proved to be extremely useful in treating electronic structure of molecules. The density functional three parameter hybrid model (DFT/B3LYP) at 6-311G(d,p)/6-311++G(d,p) basis sets level along with HF method was adopted to calculate the properties of the molecule in this work. All the calculations were performed using the Gaussian 03W program package [22] with the default convergence criteria without any constraint on the geometry [23]. It should be noted that Gaussian 03W package does not calculate the Raman intensities. The Raman activities were transformed into Raman intensities using Raint program [24] by the expression:

$$I_i = 10^{-12} \times (\upsilon_o - \upsilon_i)^4 \times 1/\upsilon_i \times RA_i \quad (1)$$

where I_i is the Raman intensity. RA_i is the Raman scattering activities, υ_i is the wavenumber of the normal modes; and υ_o denotes the wavenumber of the excitation laser [25]. For B3LYP functional, selected as the one which gives the most accurate results, calculations were continued with the expanded 6-311G(d,p) basis set. The results obtained at this level of theory, were used for the detailed interpretation of the IR and Raman spectra. TED was calculated by using the SQM program [26, 27] and the fundamental vibrational modes were characterized by their TED.

4. Results and Discussion

4.1. Molecular Geometry

Molecular structure of the title compound belongs to C_1 point group symmetry. The optimized molecular structure of 4A-N-(4MB)A is shown in Fig. 3. Optimized bond lengths, bond angles and dihedral angles of the molecule are predicted using HF/6-311++G(d,p) and B3LYP/6-311G(d,p)/6-311++G(d,p) levels are given in Table 1.

The most of the optimized bond lengths and bond angles are calculated at HF/6-311++G(d,p) and B3LYP/6-311G(d,p)/6-311++G(d,p) method correlates well with the different basis sets. The bond distance of C1-C2 is 1.401Å, 1.402 Å and 1.392 Å at B3LYP/6-311++G(d,p), B3LYP/6-311G(d,p) and HF/6-311++G(d,p) methods respectively. The reasoning of larger bond length that appears in the bond is repulsive and attractive forces of unlike charges. The maximum bond length has been calculated for C4-C16 (1.461Å), C25-C29 (1.495Å) and C29-C31 (1.519 Å) by B3LYP/6-311++G(d,p). Carbonyl group has the bond distance 1.358 Å, 1.424 Å, 1.219 Å (C1-O11, O11-C12, C29-O30 respectively).

Optimized bond angles of C2-C1-C6 are 119.8°, 119.7° and 119.7° using B3LYP/6-311++G(d,p), B3LYP/6-311G(d,p) and HF/6-31G(d,p) methods respectively. The C2-C1-O11, C25-C29-O30 bonds have different angles (124.4 and 120.8°) and this is due to the dominant ED in oxygen more than carbon and hydrogen, the C-C-H bond angle of the molecule increases and decreases towards 120 degree. Among the bond angles of O-C-H, the O11-C12-H13 has minimum angle about 111.3°. The C-C-C bond angles that end with hydrogen atom have maximum bond angle in the molecule (C2-C3-C4: 121.1°, C5-C4-C16: 122.0°, C4-C5-C6: 121.1° and C19-C21-C25: 121.0°).

Table 1. Geometric bond length, bond angle, dihedral Angle of 4AN(4MB)A

Parameters	HF/ 6-311++G(d,p)	B3LYP/ 6-311G(d,p)	B3LYP/ 6-311++G(d,p)
Bond length (Å)			
C1-C2	1.392	1.402	1.401
C1-C6	1.392	1.403	1.403
C1-O11	1.341	1.357	1.358
C2-C3	1.377	1.383	1.384
C2-H7	1.074	1.083	1.083
C3-C4	1.393	1.405	1.405
C3-H8	1.077	1.085	1.085
C4-C5	1.388	1.401	1.401
C4-C16	1.471	1.461	1.461
C5-C6	1.383	1.388	1.389
O11-C12	1.402	1.424	1.424
C16-N28	1.255	1.279	1.279
C18-C19	1.395	1.406	1.406
C18-C20	1.389	1.405	1.405
C18-N28	1.402	1.399	1.399
C19-C21	1.376	1.383	1.383
C21-C25	1.396	1.404	1.405
C23-C25	1.387	1.400	1.401
C23-H27	1.074	1.084	1.083
C25-C29	1.498	1.496	1.495
C29-O30	1.192	1.217	1.219
C29-C31	1.514	1.520	1.519
Bond Angle (°)			
C2-C1-C6	119.7	119.7	119.8
C2-C1-O11	116.0	115.8	115.8
C6-C1-O11	124.3	124.6	124.4
C1-C2-C3	119.8	119.9	119.9
C2-C3-C4	121.2	121.1	121.2
C3-C4-C5	118.4	118.4	118.4
C3-C4-C16	119.7	119.4	119.7
C5-C4-C16	121.9	121.7	122.0
C4-C5-C6	121.2	121.1	121.1
C1-C6-C5	119.7	119.7	119.7
C1-O11-C12	120.3	118.9	119.0
O11-C12-H13	111.3	111.4	111.3
C4-C16-N28	123.3	123.1	123.3
C19-C18-C20	119.1	118.7	118.7
C19-C18-N28	118.2	118.2	118.3
C20-C18-N28	122.7	123.0	122.9
C18-C19-C21	120.4	120.5	120.5
C18-C20-C23	120.2	120.4	120.4
C19-C21-C25	120.9	121.0	121.0
C20-C23-C25	121.0	120.9	121.0
C21-C25-C23	118.5	118.5	118.4
C21-C25-C29	118.7	118.4	118.7
C23-C25-C29	122.8	123.1	122.9
C16-N28-C18	119.9	120.6	120.4
C25-C29-O30	120.6	120.8	120.8
Dihedral Angle (°)			
C6-C1-C2-C3	0.0	0.0	0.0
C6-C1-C2-H7	-180.0	-180.0	-180.0
O11-C1-C2-C3	-180.0	-180.0	-180.0
O11-C1-C6-C5	180.0	180.0	180.0
C2-C1-O11-C12	-180.0	-180.0	-180.0
C1-C2-C3-H8	-180.0	-180.0	-180.0
C2-C3-C4-C16	180.0	180.0	180.0
C16-C4-C5-C6	-180.0	-180.0	-180.0
C3-C4-C16-H17	-0.1	-0.2	-0.3
C3-C4-C16-N28	178.4	178.9	178.9

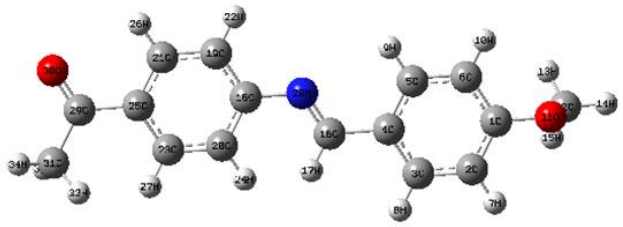

Fig 3. Optimized structure of 4A-N-(4MB)A using B3LYP/6-311G(d,p)

4.2. Potential Energy Surface Scan Studies

The PES scan on dihedral angle O_{11}-C_1-C_6-C_5 has been performed at B3LYP/6-311++G(d,p) level. The PES scan was carried out by minimizing the potential energy in all geometrical parameters by changing the torsional angle at every 10° for 360° rotation around the bond. The results obtained in PES scan study by varying the torsional perturbation around the cyanide bond (C=O) is plotted in. Fig 4. The large energy barrier of about -824.14 (Hartee) indicates that the rotation of C=O group is very much restricted.

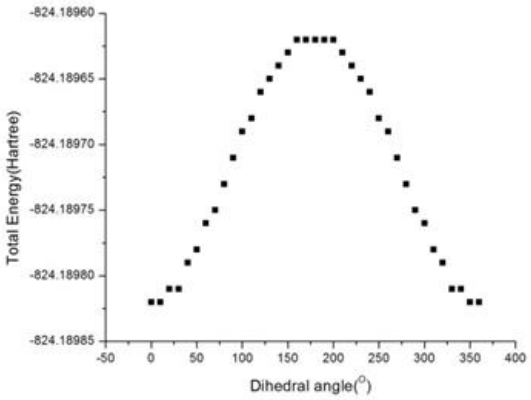

Fig 4. PES scan for dihedral angle O11-C1-C6-C5 for 4A-N-(4MB)A using B3LYP/ 6-311++G(d,p)

4.3. Vibrational Spectral Analysis

Vibrational spectral assignments were performed on the recorded FT-IR and FT-Raman spectra based on the theoretically predicted wavenumbers by *ab initio* HF/6-311++G(d,p) and DFT (B3LYP/6-311G(d,p)/6-311++G(d,p)) methods and are collected in Table-2. None of the predicted vibrational spectra has any imaginary wavenumbers, implying that the optimized geometry is located at the local lowest point on the PES. We know that *ab initio* HF and DFT potentials systematically overestimate the vibrational wavenumbers. These discrepancies are corrected either by computing anharmonic corrections explicitly or by introducing a scaled field [28] or by directly scaling the calculated wavenumbers with proper scale factors [29, 30]. After scaling with a scaling factor, the deviation from the experimental value is less than 10 cm^{-1} with few exceptions. The title molecule belongs to C_1 point group. The 96 normal modes of fundamental vibrations. Comparison of the wavenumbers calculated with experimental values reveal that the B3LYP method shows very good agreement with experimental observation due to inclusion of electron correlation for this method.

4.3.1. C-H Vibrations

In the heteroaromatic compounds, the C-H stretching vibrations normally occur at 3100-3000 cm^{-1} [31]. These vibrations are not found to be affected by the nature and position of the substituent and typically exhibit weak bands compared with the aliphatic stretching vibrations. In IR spectra, most of the aromatic compounds have nearly four peaks in the region 3080-3010 cm^{-1} due to ring C-H stretching bands. IR frequencies of C-H bands are a function of sp hybridization [32]. The scaled vibrations, [mode nos:96-83] assigned to the aromatic C-H stretch computed in the range 3375-3177 cm^{-1} and 2953-2912 cm^{-1} by B3LYP/6-311++G(d,p) method shows good agreement with the recorded medium strong FT-IR band at 3169 cm^{-1}. As expected, these fourteen modes are pure stretching modes as it is evident from TED column that they are almost contributing to 97%.

The C-H in-plane-bending vibrations are usually expected to occur in the region 1300-1000 cm^{-1} and these vibrations are very useful for characterization purposes [32]. Two medium strong peaks at 1161, 1192 cm^{-1} in FT-IR and Four very weak bands at 1272, 1273,1277, 1288 cm^{-1} in FT-IR and 1162 cm^{-1} in FT-Raman spectrum are assigned to the C-H in-plane bending vibrations. These vibrations are in good agreement with the theoretically computed values by B3LYP/6-311++G(d,p) method at 1291, 1282, 1279, 1276, 1195, 1168cm^{-1} [mode nos:57, 56, 55, 54, 51, 49]. The C-H out-of-plane bending vibrations are strongly coupled and occur in the region 1000-700 cm^{-1} [33]. Generally, the C-H out-of-plane deformation modes owned the highest wavenumbers have weaker intensity than these observing at lower wavenumbers [34]. In the title molecule 4A-N-(4MB)A, the peaks observed at 1122, 1061, 914 cm^{-1} in the FT-IR spectrum are assigned to C-H out-of-plane bending vibrations. These assignments are in good agreement with the theoretically scaled harmonic wavenumbers at 1129, 1068, 923 cm^{-1} in B3LYP/6-311++G(d,p) method [mode nos:47, 41, 36].

4.3.2. C=O Vibrations

The carbon-oxygen double bond is formed by pπ-pπ bonding between carbon and oxygen. Because of the different electro negativities of carbon and oxygen atoms, the bonding electrons are not equally distributed between the two atoms [35]. Normally, the carbonyl group vibrations occur in the region 1780-1680 cm^{-1}. In the present study, the very weak band observed at 1255 cm^{-1} in FT-Raman and strong peak observed at 1253 cm^{-1} in FT-IR is assigned to C-O stretching vibration, which is not only in well agreement with the theoretical values: 1260 cm^{-1} [mode no:53] by B3LYP/6-311++G(d,p) method, but also with literature values [30].

4.3.3. CH_3 Vibrations

In 4A-N-(4MB)A, there are two CH_3 groups attached to the benzene ring and we expect number of stretching and bending vibrations. In aromatic molecules, the asymmetric stretching vibrations of CH_3 are expected to appear in the range of 3000-2905 cm^{-1} and symmetric stretching vibrations are in the range of 2870-2860 cm^{-1} [33, 36]. In this study the harmonic frequencies 3169 and 1629 cm^{-1} (mode nos: 82 and73) by B3LYP/6-311++G(d,p) method are assigned to CH_3 asymmetric and symmetric stretching modes respectively. The in-plane bending vibrations (scissoring) of the CH_3 groups have been identified by the B3LYP/6-311G(d,p) method at 1607, 1601, 1591 cm^{-1} (mode nos:71,70,69). The CH_3 wagging vibrations computed by B3LYP/6-311G(d,p) method at 1550, 1441, 1434 cm^{-1} [mode nos:67,64,63] show good agreement with the recorded spectral value observed at 1428 cm^{-1} in FT-Raman.

Table 2. The observed FT-IR, FT-Raman and computed frequencies (cm^{-1}), IR, Raman intensities (Km/mol), reduced mass (amu) and force constants (mdyn/Å) of 4AN(4MB)A by using B3LYP/6-311++G(d,p)

Mode No.	Observed Freq. (cm^{-1})		Computed at B3LYP/6-311++G(d,p)					TED (%)
	FT-IR	FT-Raman	Freq. scaled	Intensity IR	Intensity Raman	Red. Mass	Force Const.	
υ_1			27	1.09	2.04	4.20	0.00	υ_{OC} (36%)+ t_{CCOC} (24%)
υ_2			31	1.63	9.29	5.40	0.00	t_{CCCN} (31%)+ t_{CNCC} (33%)+ t_{CCCC} (11%)
υ_3			41	0.84	1.21	4.78	0.00	t_{CNCC} (31%)+Γ_{NCCC} (12%)+Γ_{CCCC} (11%)
υ_4			63	2.01	3.11	4.10	0.01	δ_{NCC} (17%)+δ_{CNC} (15%)
υ_5			75	1.34	2.47	4.19	0.01	t_{CCCN} (10%)+ t_{CCCC} (71%)
υ_6			101	2.02	2.35	4.38	0.03	δ_{NCC} (10%)+ t_{CNCC} (19%)
υ_7			121	4.20	18.43	4.80	0.04	δ_{CCC} (10%)+ t_{CCCC} (31%)
υ_8			143	0.08	0.47	1.03	0.01	δ_{HCH} (12%)+ t_{HCOC} (12%)+ t_{CCCN} (17%)
υ_9			159	1.86	3.78	6.05	0.09	t_{HCCO} (66%)
υ_{10}			195	0.75	8.97	2.72	0.06	δ_{HCH} (14%)+ t_{HCCO} (23%)
υ_{11}			207	5.27	40.29	3.24	0.08	δ_{CCC} (43%)+δ_{CCC} (17%)
υ_{12}			239	6.58	0.72	3.62	0.12	δ_{CCC} (13%)+ t_{CCCC} (11%)
υ_{13}			241	0.25	23.11	1.51	0.05	δ_{COC} (12%)+ t_{CCCC} (10%)+ t_{CCCC} (12%)
υ_{14}	293w	294w	277	0.96	14.31	4.06	0.18	δ_{CCC} (14%)+ υ_{CC} (17%)+δ_{CCO} (11%)
υ_{15}			326	7.50	41.35	4.14	0.26	δ_{CCN} (14%)
υ_{16}			370	3.04	2.18	5.28	0.43	δ_{CCO} (22%)+ t_{CCCC} (11%)
υ_{17}	417w	418w	387	2.71	1.83	4.16	0.37	δ_{CCC} (10%)
υ_{18}			421	0.92	40.79	2.98	0.31	t_{CCCC} (24%)+ t_{CCCC} (38%)
υ_{19}			429	0.54	4.79	3.06	0.33	t_{CCCC} (46%)+ t_{CCCC} (10%)+ t_{CCCC} (21%)
υ_{20}	471w	470w	446	9.13	0.61	5.04	0.59	δ_{CCO} (18%)+δ_{COC} (10%)+δ_{CCC} (12%)
υ_{21}			468	3.41	9.92	4.29	0.55	δ_{CNC} (12%)+ t_{CNCC} (14%)
υ_{22}			505	7.63	0.58	3.44	0.52	δ_{NCC} (11%)+δ_{CCN} (14%)+δ_{CCC} (16%)
υ_{23}			530	6.17	12.10	4.05	0.67	t_{CCCC} (11%)+ t_{CCCC} (15%)+Γ_{OCCC} (11%)+Γ_{NCCC} (16%)
υ_{24}	582w	587w	543	14.22	1.70	2.74	0.47	Γ_{OCCC} (29%)+Γ_{CCCC} (26%)
υ_{25}			554	15.51	17.91	4.52	0.82	υ_{CC} (14%)+δ_{CCO} (44%)
υ_{26}	641w	639w	601	26.69	0.75	2.59	0.55	Γ_{CHCH} (14%)+Γ_{OCCC} (41%)
υ_{27}			608	56.26	12.28	3.48	0.76	δ_{CCC} (24%)+δ_{CCC} (18%)+δ_{CCC} (17%)
υ_{28}			646	2.62	13.23	7.08	1.74	δ_{CCC} (22%)+δ_{CCC} (18%)+δ_{CCC} (17%)
υ_{29}			651	0.05	2.90	6.97	1.74	δ_{CCC} (18%)+ υ_{CC} (10%)+ υ_{CC} (19%)+ υ_{CC} (13%)
υ_{30}			711	0.10	21.80	5.13	1.53	t_{CCCC} (13%)+ t_{CCCC} (17%)+ t_{CCOC} (10%)+Γ_{OCCC} (13%)
υ_{31}			736	1.34	3.60	3.71	1.18	t_{CCCC} (32%)+ t_{CCCC} (11%)+ t_{CCCC} (12%)
υ_{32}			749	0.72	4.75	3.77	1.25	δ_{CCC} (52%)
υ_{33}			786	2.44	69.89	4.34	1.58	υ_{OC} (10%)+Γ_{OCCC} (10%)
υ_{34}			825	0.77	1.70	1.26	0.50	δ_{CCC} (12%)
υ_{35}			832	15.06	58.70	1.43	0.58	υ_{CC} (12%)
υ_{36}	914ms	915w	846	41.58	15.56	1.66	0.70	t_{HCCC} (37%)+Γ_{CCCH} (18%)
υ_{37}			852	1.19	5.89	5.80	2.48	t_{HCCO} (11%)+ t_{HCCO} (16%)+ t_{HCCC} (23%)
υ_{38}			863	46.24	6.89	1.65	0.72	t_{HCCC} (17%)+ t_{HCCO} (31%)
υ_{39}			902	39.02	28.50	3.78	1.81	υ_{OC} (15%)
υ_{40}			956	80.47	70.27	2.14	1.15	Γ_{NCCC} (12%)
υ_{41}	1061w	1063w	962	0.30	8.38	1.34	0.73	υ_{CC} (32%)+Γ_{CHCH} (26%)
υ_{42}			963	1.23	22.87	1.35	0.74	t_{HCCO} (26%)+Γ_{CCCH} (38%)
υ_{43}			983	0.19	0.88	1.34	0.76	t_{HCCC} (25%)+Γ_{CCCH} (51%)
υ_{44}	1098w	1096w	1002	0.45	32.37	1.35	0.80	δ_{CCC} (14%)+δ_{CCC} (19%)
υ_{45}	1099w	1097w	1008	18.24	209.46	1.59	0.95	δ_{CCC} (11%)+δ_{CCC} (11%)
υ_{46}			1022	0.08	0.46	2.60	1.60	Γ_{CCCH} (11%)+ t_{HCCC} (37%)+ t_{HCCO} (22%)
υ_{47}	1122w	1121w	1026	5.37	14.20	2.71	1.68	t_{HCCC} (24%)+Γ_{CCCH} (54%)
υ_{48}			1043	0.74	0.27	1.88	1.20	t_{HCCC} (12%)+Γ_{CCNH} (66%)
υ_{49}	1161ms	1162w	1054	66.68	5.29	6.84	4.48	δ_{HCH} (10%)+Γ_{CHCH} (50%)+Γ_{OCCC} (17%)
υ_{50}			1089	4.13	213.55	2.46	1.72	υ_{CC} (17%)+ υ_{CC} (18%)+Γ_{CHCH} (23%)
υ_{51}	1192ms	1189w	1132	10.47	25.26	1.32	0.99	υ_{CC} (32%)+ υ_{CC} (24%)+δ_{HCC} (12%)
υ_{52}			1133	7.15	0.66	1.28	0.97	υ_{CC} (33%)+ υ_{CC} (18%)+δ_{HCC} (13%)
υ_{53}	1253w	1255w	1166	0.74	2.85	1.27	1.02	υ_{OC} (24%)
υ_{54}	1272w	1269w	1179	446.99	1565.14	1.36	1.12	υ_{CC} (11%)+ υ_{CC} (23%)+δ_{HCC} (16%)
υ_{55}	1273w	1271w	1192	18.83	185.97	1.19	1.00	δ_{HCC} (17%)+δ_{HCC} (14%)

υ_{56}	1277w	1276w	1200	7.16	5.84	1.40	1.19	υ_{CC} (10%)+ υ_{CC} (15%)+δ_{HCC} (16%)+δ_{HCC} (27%)
υ_{57}	1288w	1284w	1222	58.51	748.41	2.42	2.13	υ_{CC} (11%)+ υ_{CC} (20%)+δ_{HCC} (14%)
υ_{58}			1271	34.06	3.00	2.26	2.15	υ_{CH} (27%)
υ_{59}		1332w	1278	489.98	212.02	3.44	3.31	υ_{CC} (14%)
υ_{60}			1287	210.65	11.22	4.32	4.21	Γ_{CHOH} (32%)
υ_{61}		1377w	1320	15.64	0.46	2.08	2.13	υ_{NC} (28%)+ υ_{CC} (13%)
υ_{62}		1411w	1329	21.58	32.76	1.45	1.51	υ_{CC} (30%)+ υ_{CC} (11%)+δ_{CCO} (10%)
υ_{63}	1429w	1428w	1332	27.94	7.11	2.51	2.62	δ_{HCC} (14%)+δ_{HCC} (19%)+δ_{HCC} (20%)+δ_{HCC} (19%)
υ_{64}	1432w		1344	111.62	281.80	7.51	8.00	δ_{HCC} (17%)+δ_{HCC} (18%)+δ_{HCC} (17%)+δ_{HCC} (23%)
υ_{65}			1385	57.71	3.22	1.33	1.50	δ_{HCN} (42%)
υ_{66}	1513w		1404	5.63	132.43	1.62	1.88	δ_{HCN} (11%)+δ_{HCH} (19%)+δ_{HCH} (30%)+δ_{HCH} (16%)
υ_{67}	1543w	1542w	1441	13.57	21.19	3.09	3.79	υ_{CC} (13%)+ υ_{CC} (10%)+δ_{HCC} (12%)
υ_{68}	1557w	1559w	1453	18.31	167.17	2.86	3.56	υ_{CC} (11%)+δ_{HCN} (21%)
υ_{69}		1587w	1471	15.03	5.13	1.06	1.35	δ_{HCH} (20%)+δ_{HCH} (47%)+δ_{HCH} (16%)+Γ_{CHCH} (11%)
υ_{70}		1598w	1476	7.02	5.19	1.21	1.55	δ_{HCH} (15%)+δ_{HCH} (10%)+ t_{HCOC} (22%)+Γ_{CHOH} (17%)
υ_{71}		1061w	1480	11.62	9.94	1.05	1.35	δ_{NCH} (10%)+δ_{HCH} (30%)+δ_{HCH} (30%)
υ_{72}			1493	9.99	17.67	1.05	1.37	υ_{CH} (10%)+δ_{HCH} (40%)+ t_{CHOH} (10%)
υ_{73}	1621ms	1622w	1503	68.28	40.16	1.06	1.41	υ_{CH} (25%)+ υ_{CH} (25%)+δ_{HCH} (13%)+δ_{HCH} (21%)+ t_{HCOC} (10%)
υ_{74}			1527	0.70	252.87	2.43	3.33	δ_{HCH} (14%)
υ_{75}			1544	137.37	34.48	2.63	3.69	δ_{HCC} (10%)+δ_{HCC} (11%)+δ_{HCC} (10%)+δ_{HCC} (10%)
υ_{76}			1587	68.75	389.50	6.45	9.58	υ_{CC} (24%)+ υ_{CC} (36%)+δ_{CCC} (11%)
υ_{77}			1604	61.97	853.26	6.95	10.53	υ_{CC} (15%)+ υ_{CC} (25%)+ υ_{CC} (14%)+ υ_{CC} (18%)
υ_{78}			1623	794.72	7324.42	5.68	8.81	υ_{CC} (18%)+ υ_{CC} (21%)
υ_{79}			1646	67.28	254.55	5.78	9.22	υ_{CC} (16%)+ υ_{CC} (13%)+ υ_{CC} (12%)
υ_{80}			1687	121.93	2107.38	7.66	12.84	υ_{NC} (75%)
υ_{81}			1736	273.73	205.12	10.56	18.75	υ_{ON} (88%)
υ_{82}	3160ms	3163w	3002	39.52	57.74	1.09	5.76	υ_{CH} (11%)+δ_{HCH} (10%)+ t_{HCOC} (47%)
υ_{83}	3169ms	3167w	3012	63.10	191.52	1.03	5.53	υ_{CH} (48%)+ υ_{CH} (37%)+ υ_{CH} (14%)
υ_{84}	3192w	3194w	3033	3.47	199.98	1.04	5.62	υ_{CH} (99%)
υ_{85}			3073	32.29	65.99	1.11	6.16	υ_{CH} (14%)+δ_{HCH} (67%)
υ_{86}	3231w	3232w	3090	8.68	43.04	1.10	6.18	υ_{CH} (42%)+ υ_{CH} (51%)
υ_{87}			3140	22.24	180.47	1.10	6.39	υ_{CH} (67%)
υ_{88}	3281w	3283w	3141	16.82	150.02	1.10	6.40	υ_{CH} (10%)+ υ_{CH} (76%)
υ_{89}			3163	7.76	53.49	1.09	6.42	υ_{CH} (89%)
υ_{90}			3174	7.43	33.23	1.09	6.45	υ_{CH} (70%)+ υ_{CH} (25%)
υ_{91}			3184	2.38	47.00	1.09	6.50	υ_{CH} (85%)
υ_{92}			3191	2.22	19.80	1.09	6.53	υ_{CH} (83%)+ υ_{CH} (15%)
υ_{93}			3191	8.06	95.90	1.09	6.56	υ_{CH} (17%)+ υ_{CH} (19%)+ υ_{CH} (61%)
υ_{94}	3358w	3351w	3197	5.87	182.01	1.09	6.58	υ_{CH} (74%)+ υ_{CH} (13%)
υ_{95}			3201	2.78	136.27	1.09	6.60	υ_{CH} (89%)+ υ_{CH} (10%)
υ_{96}			3207	9.71	118.15	1.09	6.63	υ_{CH} (15%)+ υ_{CH} (84%)

ν-stretching, δ-in-plane bending, Γ-out-of-plane bending, s-strong, m-medium, w-weak, ms-medium strong, vs-very strong

Table 3. Theoretical ^{1}H and ^{13}C spectra of 4AN(4MB)A (with respect to TMS, all values in ppm)

Atoms	HF/6-311++G(d,p)	B3LYP/6-311G(d,p)	B3LYP/6-311++G(d,p)
1C	18.49	5.42	4.71
2C	65.32	55.14	54.35
3C	54.04	47.32	46.31
4C	53.43	40.62	39.54
5C	54.12	48.84	47.72
6C	63.21	53.58	52.77
12C	136.49	120.70	120.45
16C	19.99	16.89	13.85
18C	31.68	23.43	21.46
19C	61.61	50.20	49.47
20C	74.78	65.71	64.93
21C	52.07	48.29	47.09
23C	54.90	49.23	48.36
25C	51.42	39.06	37.65
29C	-27.61	-30.06	-33.48
31C	171.19	160.72	160.55
7H	24.81	24.74	24.69
8H	24.39	24.41	24.41
9H	23.00	23.27	23.17
10H	24.67	24.65	24.58
13H	29.54	29.08	29.06
14H	28.98	28.52	28.51
15H	29.58	29.11	29.06
17H	22.28	22.30	22.11
22H	24.29	24.25	24.24
24H	23.93	23.77	23.73
26H	23.24	23.59	23.48
27H	23.91	23.96	23.86
32H	30.60	30.43	30.41
33H	29.80	29.39	29.27
34H	30.30	30.38	30.45

4.3.4. Ring Vibrations

The ring carbon-carbon stretching vibrations occur in the region 1625-1430 cm^{-1}. In general, the bands are of variable intensity and are observed at 1625-1575, 1540-1470, 1465-1430 and 1380-1280 cm^{-1} from the wavenumber ranges given by Shimanouchi et al., [37] for five bands in the region. In the present investigation, the wavenumbers observed at 1559 cm^{-1} in FT-Raman and 1557 cm^{-1} in FT-IR have been assigned to C=C stretching vibration. The theoretically computed values by B3LYP/6-311G(d,p) at 1566, 1550, 1416, 1384, 1339 cm^{-1} [mode nos:68,67,62,61,59] show good agreement with experimental values. The aromatic stretching υ(c-c) vibrations give rise characteristic bands in both the observed IR and Raman spectra, covering the spectral range from 1600-1400 cm^{-1} [38-42]. The calculated harmonic mode nos: 57, 56, 51 (B3LYP/6-311++G(d,p) are in agreement with experimental FT-IR: 1288 and FT-Raman: 1284 cm^{-1} values and also find support from literature values. The C-C in-plane bending vibration calculated at 475 cm^{-1} by B3LYP/6-311G(d,p) method (mode no: 20) is in good agreement with the spectral value observed at 471 cm^{-1} in FT-IR; and the C-C out-of-plane bending vibrations are assigned to 649, 590 cm^{-1} [mode nos: 26,24] in B3LYP/6-311++G(d,p) method. Moreover, the theoretically calculated C-C-C in-plane and out-of-plane bending vibrations are in agreement with literature values [43].

5. NMR Analysis

The molecular structure of 4A-N-(4MB)A is optimized by using B3LYP method with 6-311++G(d,p). GIAO ^{13}C and ^{1}H chemical shift calculations of the title compound is made by using B3LYP method in conjunction with 6-311++G(d,p) basis set. The calculated values at different basis sets for ^{13}C and ^{1}H NMR as shown in Table 3 correlates well with each other. The ^{13}C and ^{1}H NMR spectrum of 4A-N-(4MB)A as shown in Fig. 5. The spectral value of all the atoms like Carbon, Hydrogen, Oxygen and Nitrogen shows different values for basis sets. In Carbon atome C_{31} has maximum values of 171.19, 160.72 and 160.55 by using HF/6-311++G(d,p), B3LYP/6-311G(d,p) andB3LYP/6-311++G(d,p) respectively. In Hydrogen atom H_{32} has maximum values of 30.60, 30.43, 30.46 by using HF/6-311++G(d,p), B3LYP/6-311G(d,p) andB3LYP/6-311++G(d,p) respectively. This shows that both the basis sets are in close agreement with each other.

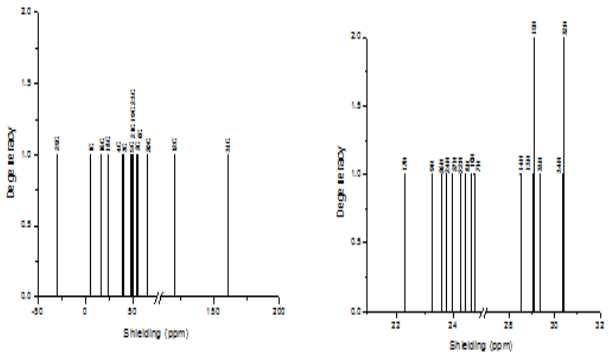

Fig 5. The computed (a) ^{1}H NMR and (b) ^{13}C NMR of 4A-N-(4MB)A

Table 4. Second order perturbation theory analysis of Fock matrix in NBO basis for 4AN(4MB)A using B3LYP/6-311G(d,p)

Donor (i)	Type	ED/e	Acceptor (j)	Type	ED/e	E(2)[a] (kJmol^{-1})	E(j)-E(i)[b] (a.u)	F(i,j)[c] (a.u)
C1-C2	σ	1.98	C1-C6	σ*	0.02	3.01	1.26	0.055
C1-C2	π	1.71	C5-C6	π*	0.03	22.59	0.28	0.072
C1-C6	σ	1.97	C1-C2	σ*	0.01	3.10	1.29	0.057
C1-C6			C6-O11		0.03	0.84	1.07	0.027
C1-H7	σ	1.98	C1-C6	σ*	0.02	0.60	1.07	0.023
C1-H7			C2-C3		0.02	4.10	1.08	0.059
C2-C3	σ	1.97	C3-C4	σ*	0.39	4.22	1.26	0.065
C2-H8	σ	1.98	C1-H7	σ*	0.01	0.67	0.96	0.023
C3-C4	σ	1.97	C3-C16	σ*	0.03	3.04	1.17	0.053
C3-C4	π	1.62	C16-N34	π*	0.16	17.56	0.28	0.066
C3-C16	σ	1.97	C3-C4	σ*	0.39	3.12	1.23	0.055
C4-C5	σ	1.97	C3-C16	σ*	0.03	3.40	1.19	0.057
C4-H9	σ	1.98	C5-H10	σ*	0.01	0.74	0.95	0.024
C5-C6	π	1.63	C5-C6	π*	0.40	0.92	0.28	0.014
C5-H10	σ	1.98	C4-H9	σ*	0.01	0.61	0.99	0.022
C6-O11	σ	1.99	C5-C6	σ*	0.40	0.97	1.46	0.034
C12-H15	σ	1.99	C6-O11	σ*	0.03	0.52	0.91	0.020
C16-H17	σ	1.99	C3-C4	σ*	0.39	4.18	1.10	0.061
C16-N34	σ	1.91	C16-H17	σ*	0.04	0.56	1.27	0.024
C18-C19	σ	1.97	C18-C20	σ*	0.03	3.86	1.24	0.062
C18-C19	π	1.60	C21-C25	π*	0.02	24.31	0.28	0.074
C18-C20	σ	1.97	C16-N34	σ*	0.16	0.73	0.72	0.021
C18-N34	σ	1.98	C3-C16	σ*	0.03	3.74	1.26	0.061
C19-C21	σ	1.98	C19-H22	σ*	0.01	1.28	1.15	0.034
C21-H26	σ	1.98	C19-C21	σ*	0.01	0.75	1.11	0.026
\C23-C25	σ	1.97	C25-C28	σ*	0.07	2.41	1.13	0.047
C23-H27	σ	1.98	C20-H24	σ*	0.01	0.74	0.95	0.024
C25-C28	σ	1.98	C23-C25	σ*	0.02	2.40	1.22	0.048
C28-O29	σ	1.97	C28-C30	σ*	0.05	0.96	1.45	0.034
C28-C30	σ	1.99	C28-O29	σ*	0.01	0.74	1.24	0.027
C30-H31	σ	1.97	C28-O29	σ*	0.14	4.65	0.54	0.046
C30-H32	σ	1.97	C28-O29	σ*	0.14	4.57	0.54	0.046
C30-H33	σ	1.99	C28-O29	σ*	0.14	1.13	1.11	0.032

[a]E(2) means energy of hyper conjugative interaction (stabilization energy)
[b]Energy difference between donor and acceptor i and j NBO orbitals.
[c]F(i,j) is the Fork matrix element between i and j NBO orbitals.

6. NBO Analysis

NBO analysis gives the accurate possible natural Lewis structure picture of ø, because all orbital are mathematically chosen to include the highest possible percentage of the ED. Interaction between both filled and virtual orbital spaces information is correctly explained by the NBO analysis. It could enhance the analysis of intra- and inter- molecular interactions. The second order Fock matrix was carried out to evaluate donor (i) – acceptor (j) i.e. donor level bonds to acceptor level bonds interaction in the NBO analysis [44]. The result of interaction is a loss of occupancy from the concentration of electron NBO of the idealized Lewis structure into an empty non-Lewis orbital. For each donor (i) and acceptor (j), the stabilization energy E(2) associates with the delocalization i → j is estimated as:

$$E(2) = \Delta E_{ij} = q_i \frac{F(i,j)^2}{\varepsilon_j - \varepsilon_i} \quad (2)$$

where q_i is the donor orbital occupancy, ε_j and ε_i are diagonal elements and F(i, j) is the off diagonal NBO Fock matrix element. NBO analysis provides an efficient method for studying intra- and inter-molecular bonding and interaction among bonds; and also provides a convenient basis for investigating charge transfer or conjugative interaction in molecular systems. Some electron donor orbital, acceptor orbital and the interacting stabilization energy resulted from the second-order micro disturbance theory are reported [45, 46].

The larger E(2) value the more intensive is the interaction between electron donors and acceptors i.e. the more donation tendency from electron donors to electron acceptors and the greater the extent of conjugation of the whole system [47]. Delocalization of ED between occupied Lewis – type (bond or lone pair) NBOs and formally unoccupied (antibond or Rydeberg) non-Lewis NBOs corresponds to a stabilizing donor- acceptor interaction. NBO analysis has been performed on the BHMBC molecule at DFT/B3LYP/6-311++G(d,p) level in order to elucidate, the intra-molecular hybridization and delocalization of ED within the molecule. The charge transfer within the molecule is more in π → π* transition. This study reveals the energy transfer during inter-molecular interactions. Transition between πC1-C2 and π*C5-C6 bonds has the energy 22.59 kJ/mol. Similarly transition between πC3-C4 and π*C16-N34 bond has the energy 17.56 kJ/mol.

The E(2) values and types of the transition for 4A-N-(4MB)A are shown in Table.4.

7. HOMO-LUMO Analysis

HOMO and LUMO are very important parameters for quantum chemistry. We can determine the way in which the

molecule interacts with other species; hence, they are called the frontier orbitals. HOMO, which can be considered as the outermost orbital containing electrons, tends to give these electrons such as an electron donor. On the other hand; LUMO can be considered as the innermost orbital containing free places to accept electrons [48]. The HOMO and LUMO energy calculated by HF/6-311++G(d,p) and B3LYP/6-311G(d,p)/6-311++G(d,p) methods are shown in Table 5. This electronic transition absorption corresponds to the transition from the ground to the first excited state and is mainly described by an electron excitation from HOMO to LUMO. In the present study, the C=C, O-CH_3 and C-O bond have highest occupied MO and the LUMO prevails over the C-C bond in 4A-N-(4MB)A. The atomic compositions of the frontier MO using B3LYP/6-311G (d,p) are shown in Fig. 6.

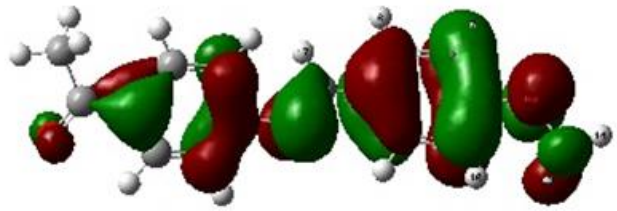

HOMO PLOT

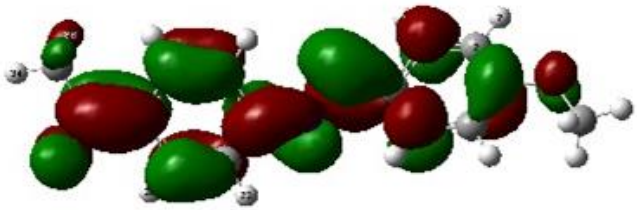

LUMO PLOT

Fig 6. The atomic orbital compositions of the frontier molecular orbital for 4A-N-(4MB)A using B3LYP/6-311++G(d,p)

Table 5. HOMO LUMO energy calculated by HF and DFT methods

Parameter	HF/ 6-311++G(d,p) (eV)	B3LYP/ 6-311G(d,p) (eV)	B3LYP/ 6-311++G(d,p) (eV)
HOMO	-0.347	-0.343	-0.343
LUMO	-0.236	-0.239	-0.239
Energy gap (ΔE)	-0.111	-0.104	-0.104

SCF energy = - 824.14 a.u.

8. Molecular Electrostatic Potential

MEP is related to the ED and is a very useful descriptor in understanding sites for electrophilic and nucleophilic reactions as well as hydrogen bonding interactions [49, 50]. The electrostatic potential *V(r)* is also well suited for analyzing processes based on the "recognition" of one molecule by another, as in drug-receptor, and enzyme-substrate interactions, because it is through their potentials that the two species first "see" each other [51, 52]. To predict reactive sites of electrophilic and nucleophilic attacks for the investigated molecule, MEP at the B3LYP/6-311++G(d,p) optimized geometry was calculated. The negative (red and yellow) regions of MEP were related to electrophilic reactivity and the positive (blue) regions to nucleophilic reactivity (Fig. 7). The negative region is localized on the oxygen atoms and the positive region is localized on the hydrogen atom. These results provide information concerning the region where the compound can interact inter-molecularly and bond metallically. Therefore, Fig. 7 confirms the non-existence of inter-molecular interactions within the molecule.

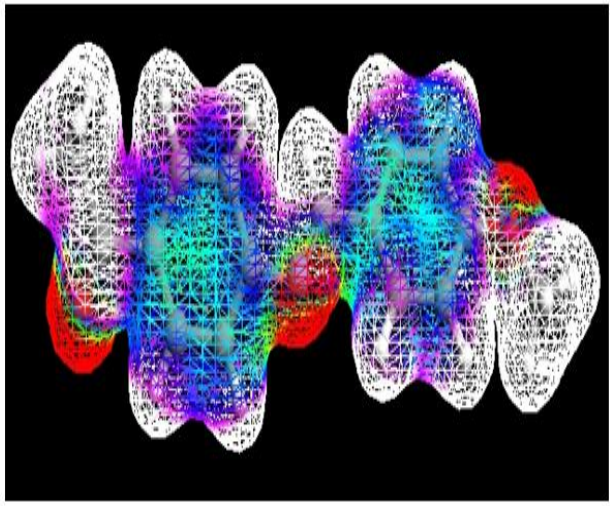

Fig. 7. Molecular electrostatic potential map calculated at B3LYP/6-311G(d,p) level for BHMBC

9. Other Molecular Properties

9.1. Mulliken Charges

The calculation of atomic charges plays an important role in the application of quantum mechanical calculations to molecular systems [53]. The charge distributions are calculated by Mulliken method [54] using HF/6-311++G(d,p), B3LYP/6-311G(d,p) and B3LYP/6-311++G(d,p) methods for the equilibrium geometry of 4A-N-(4MB)A are given in Table 6. The charge distribution on the molecule has an important influence on the vibrational spectra. The corresponding Milliken's plot is shown in Fig. 8. C_{23} possesses the most negative charges by B3LYP/6-311++G(d,p) method.

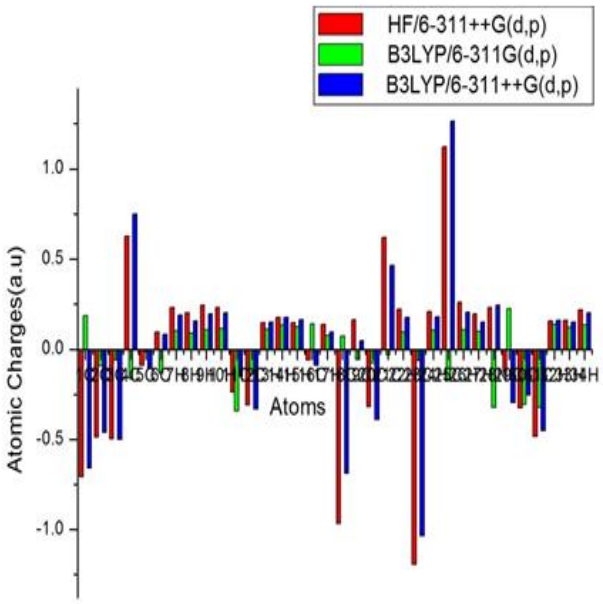

Fig. 8. Comparison of different methods for calculated atomic charges of 4A-N-(4MB)A

Table 6. Calculated Mulliken charges of 4AN(4MB)A by HF and DFT method

Charges	HF/6-311++G(d,p)	B3LYP/6-311G(d,p)	B3LYP/6311++G(d,p)
1C	-0.706	0.186	-0.658
2C	-0.489	-0.092	-0.461
3C	-0.497	-0.061	-0.501
4C	0.627	-0.162	0.748
5C	-0.088	-0.015	-0.105
6C	0.096	-0.133	0.083
7H	0.231	0.103	0.188
8H	0.202	0.088	0.158
9H	0.244	0.109	0.196
10H	0.233	0.115	0.201
11O	-0.237	-0.342	-0.151
12C	-0.311	-0.136	-0.331
13H	0.147	0.112	0.151
14H	0.176	0.134	0.177
15H	0.146	0.125	0.165
16C	-0.060	0.140	-0.088
17H	0.138	0.075	0.095
18C	-0.967	0.073	-0.688
19C	0.164	-0.056	0.047
20C	-0.318	-0.075	-0.390
21C	0.621	-0.031	0.463
22H	0.221	0.096	0.178
23C	-1.193	-0.062	-1.034
24H	0.209	0.105	0.179
25C	1.123	-0.167	1.263
26H	0.260	0.108	0.207
27H	0.195	0.098	0.151
28N	0.230	-0.323	0.243
29C	-0.124	0.225	-0.297
30O	-0.327	-0.305	-0.254
31C	-0.484	-0.324	-0.452
32H	0.156	0.137	0.162
33H	0.159	0.123	0.150
34H	**0.220**	**0.133**	**0.203**

Table 7. Theoretically computed energies, zero-point vibrational energies, rotational constants, entropies and dipole moment for 4AN(4BM)A

Parameters	HF/ 6-311++G(d,p)	B3LYP/ 6-311G(d,p)	B3LYP/ 6-311++G(d,p)
Total Energies (a.u)	-818.74	-823.91	-823.92
Zero point energy (kcal/mol)	182.24	170.44	170.20
Rotational constants (GHz)	1.94	1.90	1.90
	0.10	0.10	0.10
	0.10	0.10	0.10
Entropy (cal/mol/K)			
Total	133.36	136.76	137.58
Translational	42.49	42.49	42.49
Rotational	34.02	34.06	34.06
Vibrational	56.85	60.22	61.04
Dipole moment (D)	5.34	5.79	5.81

9.2. Thermodynamic Properties

The calculated thermodynamic parameters are presented in the Table 7. Scale factors have been recommended [55] for an accurate prediction in determining the zero-point vibrational energies and the entropy S. The variations in the zero-point vibrational energies seem to be insignificant. The total energies found to decrease with increase of the basis sets. The changes in the total entropy of 4A-N-(4MB)A at room temperature at different basis sets are only marginal.

10. Conclusion

A complete vibrational and molecular structure analysis has been performed based on the quantum mechanical approach by *ab initio* HF and DFT (B3LYP) calculations. NBO reflects the charge transfer within the molecule. HOMO and LUMO orbitals have been visualized. ^{13}C and ^{1}H NMR chemical shifts calculation of the 4A-N-(4MB)A molecule were carried out by using B3LYP functional with 6-311G(d,p) basis set and the result coincide well with the different basis sets. Moreover, MEP, several thermodynamic properties and Mulliken charges are also calculated.

References

[1] D.J. Creighton, Z.B. Zheng, R. Holewinski, D.S. Hamilton, J.L. Eiseman, Glyoxalase I inhibitors in cancer chemotherapy, Biochem. Soc. 31 (2003) 1378.

[2] A. Goel, A.B. Kunnumakkara, B.B. Aggarwal, Curcumin as "Curecumin": from kitchen to clinic, Biochem. Pharmacol. 75 (2008) 787.

[3] T. Santel, G. Pflug, N.Y.A. Hemdan, A. Schäfer, M. Hollenbach, Curcumin inhibits glyoxalase 1-a possible link to its anti-inflammatory and anti-tumor activity, PLoS ONE, 3(2008) e3508.

[4] R.C. Srimal, B.N. Dhawan, Pharmacology of diferuloyl methane (curcumin), a nonsteroidal antiinflammatory agent, J. Pharm. Pharmacol. 25 (1972) 447.

[5] O.P. Sharma, Antioxidant activity of curcumin and related compounds, Biochem. Pharmacol. 25 (1976) 1811.

[6] S.C. Sharma, H. Mukhtar, S.K. Sharma, M. Krishna, Lipid peroxide formation in experimental inflammation, Biochem. Pharmacol. 21 (1972) 1210.

[7] A. Mukopadhyay, N. Basu, N. Ghatak, P.K. Gujral, Anti-inflammatory and irritant activities of curcumin analogues in rats, Agents Actions 12 (1982) 508.

[8] T. Kosuge, H. Ishida, H. Yamazaki, Studies on active substances in the herbs used for oketsu ("stagnant blood") in Chinese medicine. III. On the anticoagulative principles in curcumae rhizome, Chem. Pharm. Bull. (Tokyo) 33 (1985) 1499.

[9] H.H. Tonnesen, Ph.D. Thesis, Institute of Pharmacy, University of Oslo, Norway (1986).

[10] J. Deli, T. Lorand, D. Szabo, A. Foldesi, Potentially bioactive pyrimidine derivatives. 1. 2-Amino-4-aryl-8-arylidene-3,4,5,6,7,8-hexahydroquinazoline, Pharmazie 39 (1984) 539.

[11] G.K. Kaushal, Synthesis and characterization of photo-cross-linkable main- chain liquid-crystalline polymers containing bis benzylidene cycloalkanone units, Polymer 36 (1995) 1903.

[12] A.G. Griffin, J.F. Johnson, Liquid Crystals and Ordered Fluids, New York, Plenum Press, (1984).

[13] A. Blumstein, Polymeric Liquid Crystals, New York, Plenum Press, (1985).

[14] L.L. Chapoy, Recent Advances in Liquid Crystalline Polymers, London, Elsevier (1986).

[15] J. Kawamata, K. Inove, T. Inabe, M. Kiguchi, M. Kato, Y. Taniguchi, Large second-harmonic generation coefficients of bis(benzylidine) cycloalkanones estimated by the second-harmonic wave generated with the evanescent wave technique, Chem. Phys. Lett. 249 (1996) 29.

[16] M. Ogawa, Y. Ishii, T. Nakno, S. Irifune, Jpn. Kohai Tokyo. Chem. Abstr. 63 (1988) 238034.

[17] V.D. John, G. Kuttan, K. Krishnankutty, Anti-tumour studies of metal chelates of synthetic curcuminoids, J. Exp. Clin. Cancer. Res. 21 (2002) 219.

[18] M.O. Iwunze, Fluorescence Quenching Studies of Curcumin by Hydrogen Peroxide in Acetonitrile Solution, Monatshefte für Chemie 135 (2004) 231.

[19] Enrico Benassi and Ferdinando Spagnolo, A theoretical study about the structural, electronic and spectroscopic properties of the ground and singlet excited states of curcuminoidic core, Theoretica Chimica Acta 124 (2009) 235.

[20] Bahjat A. Saeed, Kawkab Y. Saour, Rita S. Elias, Arkivoc, The Investigation of NMR Spectra of Dihydropyridones Derived from Curcumin, ARKIVOC (xiii) (2009) 42.

[21] Yukio Murakami, Hiroaki Ishii, Naoki Takada, Shoji Tanaka, Mamoru Machino, Shigeru Ito, SeiichiroFujisawa, Comparative Anti-inflammatory Activities of Curcumin and Tetrahydro curcumin Based on the Phenolic O-H Bond Dissociation Enthalpy, Ionization Potential and Quantum Chemical Descriptor, Anticancer Res. 28 (2008) 699.

[22] Gaussian 03W program, (Gaussian Inc. Walling ford CT) (2004).

[23] H.B. Schlegel, Optimization of equilibrium geometries and transition structures, J. Comput. Chem. 3 (1982) 214.

[24] D. Michalska, Raint Program, Wroclaw University of Technology, (2003).

[25] D. Michalska, R. Wysokinski, The prediction of Raman spectra of Platinum (II) anticancer drugs by density functional theory, Chem. Phys. Lett. 403 (2005) 211.

[26] J. Baker, A.A. Jarzecki, P. Pulay, Direct scaling of primitive value Force Constants: An alternative Approach to scaled Quantum Mechanical Force fields, J. Phys. Chem. 102A (1998) 1412.

[27] P. Pulay, J. Baker, K. Wolinski. 2013 Green Arc Road, Suite A, Fayettevile, AR72703, USA.

[28] P. Pulay, G. Fogarasi, G. Pongor, J.E. Boggs, A.Vargha, Combination of Theoretical *ab initio* and Experimental Information to Obtain Reliable Harmonic Force Constants. Scaled Quantum Mechanical Force Fields for Glyoxal, Acrolein, Butadiene, Formaldehyde, and Ethylene, J. Am. Chem. Soc. 105 (1983) 7037.

[29] A.P. Scott, L. Radom, Harmonic Vibrational Frequencies: An Evaluation of Hartree-Fock, Møller-Plesset, Quadratic Configuration Interaction, Density Functional Theory, and Semiempirical Scale Factors, J. Phys. Chem. 100 (1996) 16502.

[30] Isa Sidir, Yadigar Gulseven Sidir, Mustafa Kumalar, Erol Tasal, *Ab initio* Hartree-Fock and density functional theory investigations on the conformational stability, molecular structure and vibrational spectra of 7-acetoxy-6-(2,3-dibromopropyl)-4,8-dimethylcoumarin molecule, J. Mol. Struct. 964 (2010) 134.

[31] B. Stuart, Infrared Spectroscopy: Fundamentals and Applications, John Wiley & Sons, Ltd., January, (2008).

[32] D.L. Pavia, G.M. Lampman, G.S. Kriz, Physics Editor: J. Vondeling, Introduction to Spectroscopy: A guide for student

of organic chemistry, Third Edition, Thomson Learning, (2001), p.579.
[33] N.P.G. Roeges, A Guide to the Complete Interpretation of Infrared Spectra of Organic Structures, Wiley, New York, (1994).
[34] K.R. Ambujakshan, V.S. Madhavan, H.T. Varghese, C.Y. Panicker, O. Temiz-Arpaci, B. Tekiner-Gulbas, I. Yildiz, Vibrational spectroscopic studies and *ab initio* calculations of 5-methyl-2-(*p*-methylaminophenyl) benzoxazole, Spectrochim. Acta 69A (2008) 782.
[35] J. Karpagam, N. Sundaraganesan, S. Sebastian, S. Manoharan, M. Kurt, Molecular structure, vibrational spectroscopic, first-order hyperpolarizability and HOMO, LUMO studies of 3-hydroxy-2-naphthoic acid hydrazide, J. Raman Spectrosc. 41 (2010) 53.
[36] N.B. Colthup, L.H. Daly, S.E. Wiberly, Introduction to Infrared and Raman Spectroscopy, 3rd ed, Academic press, Boston, (1990).
[37] T. Shimanouchi, Y. Kakiuti, I. Gamo, out-of-plane CH Vibrations of Benzene Derivatives, J. Chem. Phys, 25 (1956) 1245.
[38] N.P. Sing, R.A. Yadav, Vibrational studies of trifluoromethyl benzene derivatives I: 2- amino-5-chloro and 2- amino-5-bromo benzotrifluorides, Ind. J. Phys. B 75 (2001) 347.
[39] V. Krishnakumar, R. John Xavier, Density functional theory calculations and vibrational spectra of 3,5-dibromopyridine and 3,5-dichloro-2,4,6-trifluoropyridine, Spectrochim. Acta 61A (2005) 253.
[40] D.A. Prystupa, A. Anderson, B.H. Torrie, Raman and infrared study of solid benzyl alcohol, J. Raman Spectrosc. 25 (1994) 175.
[41] R.K. Yadav, N.P. Singh, R.A. Yadav, Vibrational studies of trifluoromethyl benzene derivatives II: 5-amino-2-fluoro and 5-amino-2-chloro benzotrifluorides, Ind. J. Phys. B 77 (2003) 419.
[42] D.N. Sathyanarayana, Vibrational Spectroscopy, Theory and Applications, New Age International Publishers, New Delhi, (2004).
[43] M. Karabacak, M. Cinar, S. Ernec, M. Kurt, Experimental vibrational spectra (Raman, infrared) and DFT calculations on monomeric and dimeric structures of 2- and 6- bromonicotinic acid, J. Raman Spectrosc. 41 (2010) 98.
[44] M. Szafran, A. Komasa, E.B. Adamska, Crystal and molecular structure of 4-carboxypiperidinium chloride (4-piperidinecarboxylic acid hydrochloride, J. Mol. Struct. 827 (2007) 101.
[45] C. James, A. Amal Raj, R. Rehunathan, V.S. Jayakumar, I.H. Joe, Structural conformation and vibrational spectroscopic studies of 2,6-bis(p-N,N-dimethyl benzylidene) cyclohexanone using density functional theory, J. Raman Spectrosc. 37 (2006)1381.
[46] L. Jun-na, C. Zhi-rang, Y. Shen-fang, J. Zhejiag, Study on the prediction of visible absorption maxima of azobenzene compounds, Univ. Sci. 6B (2005) 584.
[47] S. Sebastian, N. Sundaraganesan, The spectroscopic (FT-IR, FT-IR gas phase, FT-Raman and UV) and NBO analysis of 4-Hydroxypiperidine by density functional method, Spectrochim. Acta 75A (2010) 941.
[48] G. Gece, The use of quantum chemical methods in Corrosion inhibitor studies, Corros. Sci. 50 (2008) 2981.
[49] E. Scrocco, J. Tomasi, Electronic Molecular Structure, Reactivity and Inter-modular Forces: An Euristic Interpretation by Means of Electrostatic Molecular Potentials, Adv. Quantum. Chem. 11 (1978) 115.
[50] E.J. Luque, J.M. Lopez, M. Orozco, Electrostatic interactions of a solute with a continuum. A direct utilization of *ab initio* molecular potentials for the prevision of solvent effects, Theor. Chem. Acc. 103 (2000) 343.
[51] P. Politzer, P.R. Laurence, K. Jayasuriya, Molecular electrostatic potentials: an effective tool for the elucidation of biochemical phenomena, J. Environ. Health Perspect, 61 (1985) 191.
[52] E. Scrocco, J. Tomasi, Top. Curr. Chem. 7 (1973) 95.
[53] S. Gunasekaran, S. Kumaresan, R. Arunbalaji, G. Anand, S. Srinivasan, Experimental and theoretical investigations of spectroscopic properties of N-acetyl-5-methoxytryptamine, J. Chem. Sci. 120 (2008) 315.
[54] R.S. Mulliken, Electronic Population Analysis on LCAO-MO Molecular Wave Functions, J. Chem. Phys. 23 (1955) 1833.
[55] M.A. Palafox . Scaling factors for the prediction of vibrational spectra. I. Benzene molecule, Int. J. Quantum. Chem. 77 (2000) 6.